Data-driven modeling of broadband trailing-edge noise

27th International Congress
on Sound and Vibration
The annual congress of
the International Institute
of Acoustics and Vibration (IIAV)

11-16 July, 2021

ICSV27

Annual Congress of the International Institute of Acoustics and Vibration (IIAV)

DATA-DRIVEN MODELING OF BROADBAND TRAILING-EDGE NOISE

Renzo Arina
Politecnico di Torino, Torino, Italy
e-mail: renzo.arina@polito.it
Andrea Ferrero
Politecnico di Torino, Torino, Italy
email: andrea_ferrero@polito.it

The broadband noise emitted at the trailing edge of an airfoil represents a significant contribution to the noise emission of several industrial components, in both energy and aeronautical fields. Several analytical models focus the attention on some features of the boundary layer close to the trailing edge and use this information to predict the emissions. However, the prediction capability of these models is limited since they are based on several simplifying assumptions. Recently, research efforts have been devoted to the development of machine learning techniques which make it possible to analyze large amounts of experimental data in order to automatically extract modeling knowledge.
In this work, Artificial Neural Networks (ANNs) are proposed as empirical models to describe the wall pressure spectrum and the noise directivity. First of all, a study on the choice of the ANN architecture is performed. In order to accomplish this task, an artificial database is generated by using existing semi-empirical models for the prediction of the wall pressure spectrum at different angles of attack: this makes it possible to identify the minimum complexity that the ANN should have in order to accurately describe the spectrum. A second ANN is trained on the directivity distribution obtained by the Amiet analytical theory: both shallow and deep architectures are investigated.
The motivation of the present work lies in the fact that the existing analytical models used for building the artificial database are fairly good approximations of the physical phenomena: this means that the chosen ANN architecture is sufficiently complex to accurately describe also a measured noise emission which should represent a perturbation with respect to the models. In this way it is possible to improve the prediction ability of the ANN model by enriching the database with experimental data: this would lead to a general model which is not limited by the simplifying assumptions on which the analytical theories are based.

Keywords: trailing-edge noise, broadband noise, machine learning, data-driven model

1. Introduction

The broadband noise emitted at the trailing edge of an airfoil represents a significant contribution to the noise emission of wing and blade profiles. In particular, there is great interest in the study of the mechanisms which control this phenomenon because they can be exploited to reduce the noise emission from wind turbines, fans and open-rotor engines. In particular, several studies showed that the broadband trailing-edge noise represents a significant contribution to the noise emitted by open-rotor engines [1].

Several research efforts have been devoted to the development of techniques for reducing this noise contribution. Among them, trailing-edge serrations show promising results for both wings and rotating blades [2, 3, 4]. The source of the trailing-edge noise is related to the diffraction of turbulence in the boundary layers and in the near wake by the trailing edge. For this reason, models focus the attention on some features of the boundary layer close to the trailing edge and use this information to predict the wall pressure spectrum which determines the magnitude of the emitted noise. In particular, the knowledge of the wall pressure spectrum allows to define an equivalent point source located at the trailing edge: the propagation can then be computed by means of the Amiet analytical theory. However, the prediction capability of the Amiet model is limited since it is based on several simplifying assumptions and so it does not take into account some features of the airfoil (curvature, thickness,...).

Recently, several research efforts have been devoted to the development of machine-learning techniques which make it possible to analyze large amounts of experimental data in order to automatically extract modeling knowledge. These techniques, which have been recently developed in the field of turbulence modeling [5, 6, 7], can be used to find correlations hidden in the experimental data and to provide correction terms which can improve existing models. Tracey et al. [8] performed a study in which an Artificial Neural Network (ANN) is used to reproduce the source term of the Spalart-Allmaras turbulence closure. The aim of the work was not to improve the predictive capability of the original model: the goal was to verify the possibility of describing the source term by an ANN.

In the present work, an approach which follows the same spirit is applied to the modeling of the broadband trailing-edge noise emission. In particular, an artificial database for the trailing-edge noise emitted by a NACA0012 airfoil in several working conditions is generated: the database is computed by using existing semi-empirical models of the wall pressure spectrum and the Amiet theory for the propagation.

These models are able to predict the trend and the order of magnitude of the emitted noise but there are several discrepancies between the different models. However, they represent a reasonable representation of the phenomenon. For this reason, the artificial database is used to choose the architecture of two ANNs which describe the wall pressure spectrum and the directivity.

This approach is general and can be applied to several problems. The basic idea is that the prediction of the models used to choose the architecture of the ANN are not too far from the experimental results: if this condition is satisfied, then the chosen ANN is sufficiently general to capture the correlations hidden in the experimental data and so can potentially lead to a more general and accurate model.

2. Analytical model for broadband trailing edge noise

When the unsteady vortical structures in the boundary layers, on the pressure and suction side of a lifting surface, interacts with the sharp corner present at the trailing edge, noise generation occurs.

The noise source is the boundary-layer turbulence convected over the trailing edge, therefore trailing-edge noise can be described in terms of the Lighthill's acoustic analogy. A first solution of the Lighthil's equation was provided by Ffwocs Williams and Hall [9], for a semi-infinite flat plate, employing a tailored Green's function chosen to satisfy the no-slip boundary condition on the plate. Amiet [10] solved the Curle's equation and developed an analytical approach to the quantitative prediction of the trailing-edge noise. Both approaches rely on the thin-airfoil approximation in a uniform flow, assuming a semi-infinite flat plate in upstream direction.

For a wing of high aspect ratio, the noise perceived by an observer located in the mid span plane is

described by the power spectral density for a given frequency ω and position $\mathbf{x} = (y = 0, R, \theta)$

$$S_{pp}(\mathbf{x}, \omega) = 2 \left(\frac{\omega c z}{4\pi c_0 \sigma^2} \right) L \, | \mathcal{L}(\omega, \theta) |^2 \, \ell_y(\omega) \Phi_{pp}(\omega) \, , \tag{1}$$

where c is the chord, L the plate span, $\mathcal{L}(\omega, \theta)$ the aeroacoustic transfer function [11], $\sigma^2 = x^2 + \beta^2(y^2 + z^2)$, $\beta^2 = 1 - M^2$ with M the Mach number of the uniform stream and c_0 the speed of sound. $\ell_y(\omega)$ is the spanwise correlation length given by the Corcos model $\ell_y(\omega) = 1.2 U_c / \omega$, being U_c the convection velocity. $\Phi_{pp}(\omega)$ is the wall pressure spectrum.

Formula (1) provides the scaling and directivity properties of the trailing-edge noise. A more detailed description requires an estimate of the wall pressure spectrum describing the turbulent structure of the boundary layer near the trailing edge. A semi-empirical wall pressure spectrum is represented by the relation

$$\Phi_{pp} = \frac{\widetilde{\Phi}_{pp}}{\Phi^*} = \frac{a \widetilde{\omega}^b}{\left(i \widetilde{\omega}^c + d \right)^e + \left(f R_T^g \widetilde{\omega} \right)^h} \, . \tag{2}$$

Where $\widetilde{\omega} = \omega \delta^* / U_e$, $R_T = \delta^* \tau_w / (U_e \mu)$ and $\Phi^* = \tau_w^2 \delta^* / U_e$. δ^* is the boundary-layer displacement thickness and τ_w the wall shear stress. Defining the Zagarola-Smith parameter $\Delta = \delta / \delta^*$, the Clauser's equilibrium parameter $\beta_c = (\theta / \tau_w)(dp/dx)$ and the Coles' wake function $\Pi = 0.8(\beta_c + 0.5)^{3/4}$, in the Rozenberg model [12] the parameters are defined as: $a = [2.82\Delta^2 (6.13 * \Delta^{-0.75} + d)^e][4.2\Pi/\Delta + 1]$, $b = 2.0$, $c = 0.75$, $d = 4.76(1.4/\Delta)^{0.75}(0.375e - 1)$, $e = 3.7 + 1.5\beta_c$, $f = 8.8$, $g = -0.57$, $h = min(3, 19/\sqrt{R_T}) + 7$, $i = 4.76$. In the Kamruzzaman [13] model the parameters are: $a = 0.45[1.75(\Pi/\beta_c)^{2m} + 15]$, $m = 0.5[(\delta^*/\theta)/1.31]^{0.3}$, $b = 2.0$, $c = 1.637$, $d = 0.27$, $e = 2.47$, $f = 1.15^{-2/7}$, $g = -2/7$, $h = 7$ and $i = 1$.

A rectangular wing of span $L = 1\,m$ with NACA0012 airfoil of chord $c = 0.4\,m$, at Reynolds number $Re = 1.5 \cdot 10^6$, at different angles of attack ($\alpha = 0°, 4°, 6°$) is considered. The wall pressure spectra obtained by the models of Rozenberg [12] and Kamruzzaman [13] are compared to the experimental results of IAG reported in [14]. The boundary-layer properties required by the models are evaluated by means of the XFoil tool [15]. An example of wall pressure spectrum for the suction side is reported in Figure 1a. This spectrum determines the magnitude of the noise source that can be propagated by means of the Amiet expression (1): an example of the far-field noise spectrum evaluated at $R = 1\,m$, $\theta = 90°$ from the trailing edge is reported in Figure 1b.

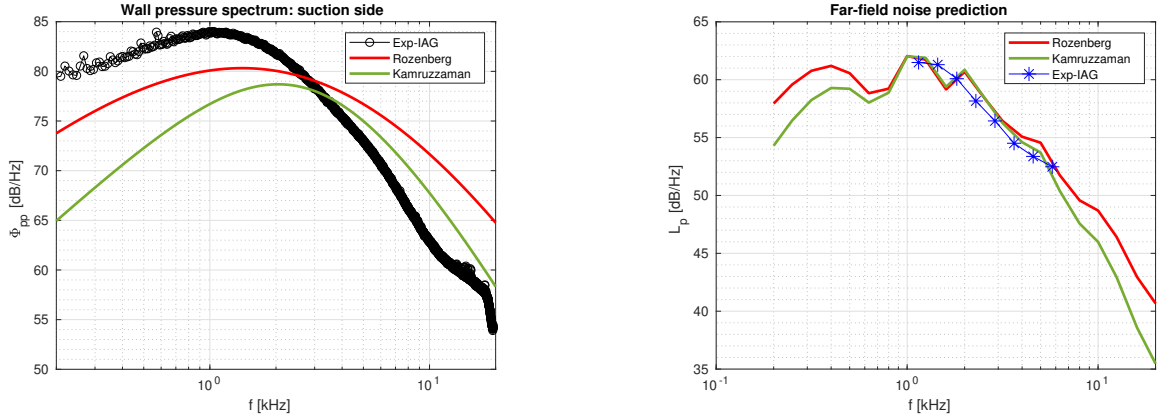

(a) Wall pressure spectrum for suction side

(b) Spectrum of far field noise

Figure 1: NACA0012, chord $c = 0.4\,m$, $\alpha = 4°$, $Re = 1.5\,10^6$

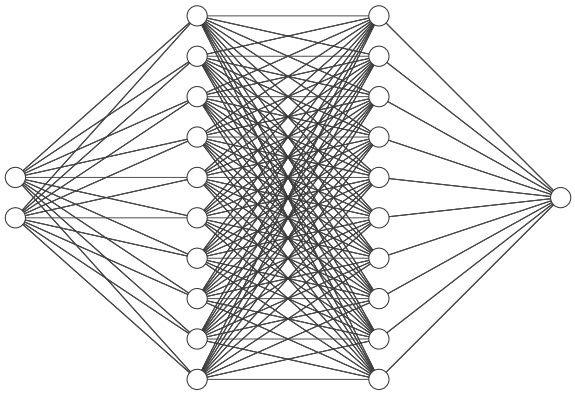

(a) ANN architecture

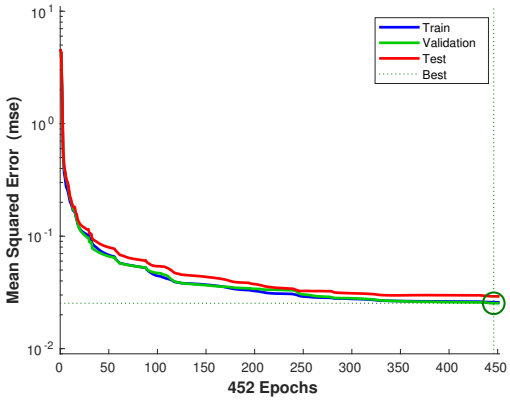

(b) Training history

Figure 2: Example of ANN

3. ANN-based wall pressure spectrum

First of all, a database of the wall pressure spectrum computed by Rozenberg and Kamruzzaman models is computed at $\alpha = 0°, 4°, 6°$. In particular, it is chosen to devote the database to the description of the pressure side wall pressure spectrum. Since the airfoil is symmetric, the suction side results are equivalent to the pressure side results for opposite angles of attacks and so the database contains the results for $\alpha = 0°, \pm 4°, \pm 6°$.

An ANN with two inputs (angle of attack and frequency) and one output (wall pressure spectrum on the pressure side) is introduced. An example of such a network is reported in Figure 2a. Sigmoid activation functions are used of the the neurons in the hidden layers while a linear activation function is used in the output layer. The training of the ANN network is performed in Matlab with the Levenberg-Marquadt algorithm: the training is performed by dividing randomly the database in 3 subsets (training, validation and test) in order to avoid overfitting. An example of training history is reported in Figure 2b. The ability of the network to fit the data in the training, validation and test data sets is evaluated by means of regression plots which show the reference value and the predicted value on the two axis, as shown in Figure 3. The regression coefficient R obtained for the fitting of the different analytical models by different ANN architectures is reported in Table 1 and 2. Since the functional form of the wall pressure spectrum is quite simple it is sufficient to introduce a few neurons in the ANN to describe accurately the database: a network with a hidden layer with just four neurons is chosen. The same architectures are then used to fit the experimental data from [14] and show a reasonable fitting, as reported in Table 3.

Layers	Neurons per layer	Regression coeff. R
1	1	0.990
1	2	0.995
1	4	1.000

Table 1: Choice of the ANN architecture for wall pressure spectrum (Rozenberg)

Layers	Neurons per layer	Regression coeff. R
1	1	0.975
1	2	0.987
1	4	1.000

Table 2: Choice of the ANN architecture for wall pressure spectrum (Kamruzzaman)

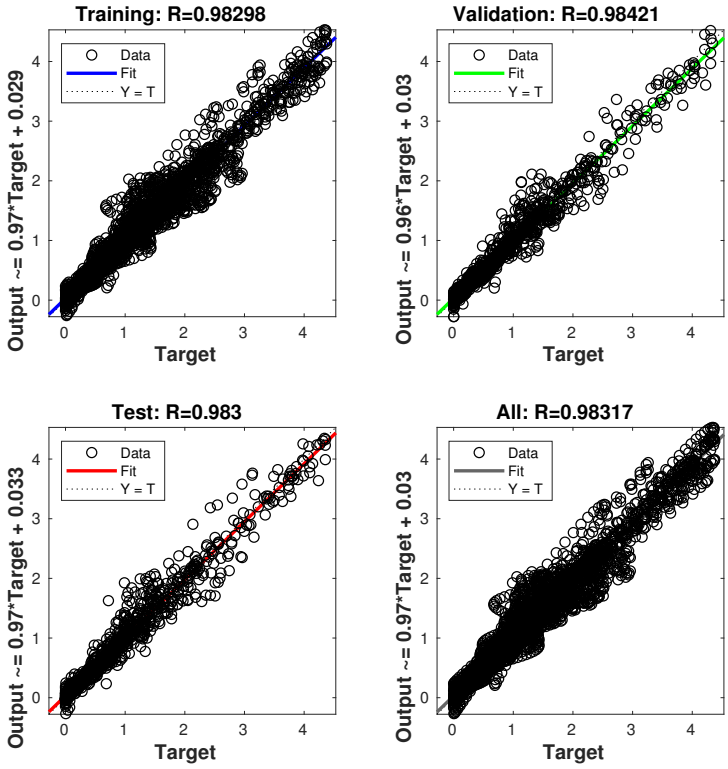

Figure 3: Regression plot for training, validation, test and full dataset

Layers	Neurons per layer	Regression coeff. R
1	1	0.929
1	2	0.965
1	4	0.995

Table 3: Choice of the ANN architecture for wall pressure spectrum (Experimental results)

4. ANN-based directivity

The Amiet theory [10] allows to compute the propagation of the noise in the different directions identified by the angle θ. The directivity pattern is strongly influenced by the noise frequency: this makes the fitting of the results significantly more challenging. An ANN with two inputs (frequency f and direction θ) and one output (the sound pressure level normalised with respect to the value at $\theta = 90°$ is considered. A database is generated by dividing the frequency range $10^2 Hz \leq f \leq 10^4 Hz$ in 20

intervals with logarithmic scaling. The directivity distribution with respect to the angle θ is discretized by steps of 1°. The obtained database is used to investigate the ANN's architecture requirements. In Table 4 the regression coefficient R for different networks is reported. A first set of tests is performed by using shallow networks with just one hidden layer and increasing the number of neurons. A second set of tests is performed by using deep networks with a different number of hidden layers and 10 neurons per layer. The results show that the deep networks allow to better fit the database with respect to the corresponding shallow networks with the same total number of neurons.

Finally, a prediction test is performed by using the ANN to evaluate the directivity pattern at $f = 350$ Hz and $f = 4500$ Hz. These tests represent actual predictions since these frequency values are not included in the training database, the closest values are 316 Hz and 398 Hz for the first, and 3981 Hz and 5012 Hz for the second. The plots in Figure 4 show a comparison between the reference directivity pattern, computed by the Amiet theory, and the results obtained by a shallow ANN (1×160) and a deep ANN (16×10) with the same total number of neurons: the deep network outperforms the shallow one. A similar trend is observed in the plots of Figure 5 which refer to the prediction at $f = 4500$ Hz.

Layers	Neurons per layer	Regression coef. R
1	10	0.891
1	20	0.932
1	40	0.965
1	80	0.984
1	160	0.992
2	10	0.983
4	10	0.997
8	10	0.999
16	10	0.999

Table 4: Choice of the ANN architecture for directivity fitting

(a) ANN 1x160

(b) ANN 16x10

Figure 4: Directiviy prediction for $f = 350$ Hz

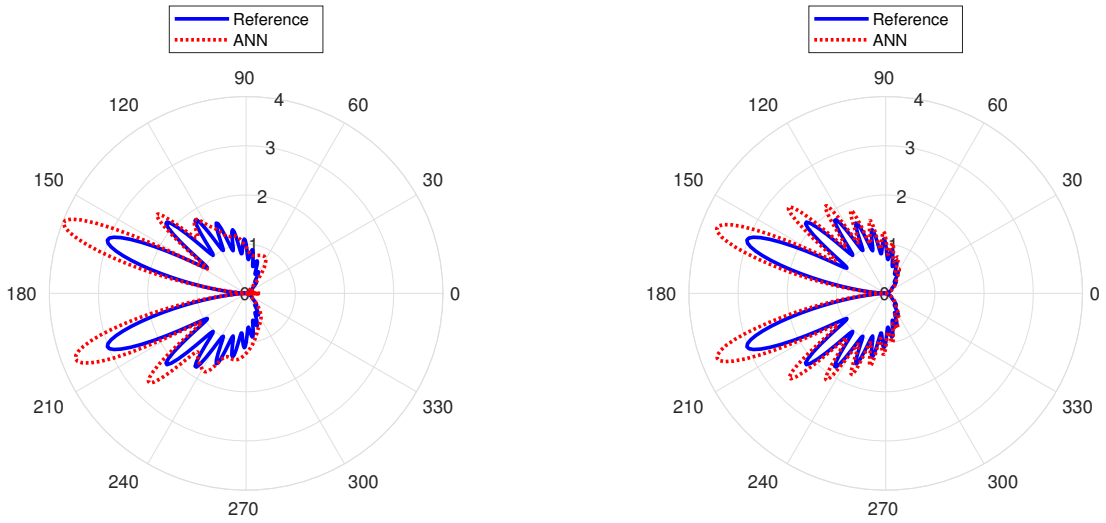

(a) ANN 1x160 (b) ANN 16x10

Figure 5: Directiviy prediction for $f = 4500$ Hz

5. Conclusions

The use of ANNs for the description of the wall pressure spectrum and the directivity pattern of the broadband trailing-edge noise was investigated. The tests showed that ANNs can easily describe the wall pressure spectrum while the approximation of the directivity pattern is significantly more challenging, due to its strong dependency on frequency. It was found that deep neural networks can outperform shallow networks in this kind of application. The results presented in this work were obtained by generating an artificial database by means of the Kamruzzaman and Rozenberg models for the wall pressure spectrum and the Amiet theory for noise propagation. The ability of the ANNs to reproduce the results of these models paves the way to the development of data-driven models for broadband trailing-edge noise in which the networks are directly trained on experimental data. In this way it would be potentially possible to obtain general models which could take into account several features of the airfoil (curvature, thickness,...) without the need to adopt the simplifying assumptions on which the Amiet theory is based (flat plate approximation).

REFERENCES

1. Kingan, M. Advanced open rotor noise prediction, *The Aeronautical Journal*, **118** (1208), 1125–1135, (2014).

2. Howe, M. S. Aerodynamic noise of a serrated trailing edge, *Journal of Fluids and Structures*, **5** (1), 33–45, (1991).

3. Gruber, M., Joseph, P. and Chong, T. P. Experimental investigation of airfoil self noise and turbulent wake reduction by the use of trailing edge serrations, *16th AIAA/CEAS aeroacoustics conference*, p. 3803, (2010).

4. Finez, A., Jacob, M., Roger, M. and Jondeau, E. Broadband noise reduction of linear cascades with trailing edge serrations, *17th AIAA/CEAS Aeroacoustics Conference (32nd AIAA Aeroacoustics Conference)*, p. 2874, (2011).

5. Wu, J.-L., Xiao, H. and Paterson, E. Physics-informed machine learning approach for augmenting turbulence models: A comprehensive framework, *Physical Review Fluids*, **3** (7), 074602, (2018).

6. Duraisamy, K., Iaccarino, G. and Xiao, H. Turbulence modeling in the age of data, *Annual Review of Fluid Mechanics*, **51**, 357–377, (2019).

7. Sandberg, R. D. and Michelassi, V. The current state of high-fidelity simulations for main gas path turbomachinery components and their industrial impact, *Flow, Turbulence and Combustion*, **102** (4), 797–848, (2019).

8. Tracey, B. D., Duraisamy, K. and Alonso, J. J. A machine learning strategy to assist turbulence model development, *53rd AIAA aerospace sciences meeting*, p. 1287, (2015).

9. Ffowcs Williams, J. and Hall, L. Aerodynamic sound generation by turbulent flow in the vicinity of a scatering half plane, *J. Fluid Mech.*, **40**, 657–670, (1970).

10. Amiet, R. Effect of incident surface pressure field on noise due to turbulent flow past a trailing edge, *J. Sound Vib.*, **57**, 305–306, (1978).

11. Roger, M. and Moreau, S. Back-scatterng correction and further extensions of amiet's trailing-edge noise model. part 1: theory, *J. Sound Vib.*, **286**, 477–506, (2005).

12. Rozemberg, Y., Robert, G. and Moreau, S. Wall-pressure sectral model including the adverse pressure gradient effects, *AIAA J.*, **50-12**, 2168–2179, (2012).

13. Kamruzzaman, M., Bekiropoulos, D., Lutz, T., Wurz, W. and Kramer, E. A semi-empirical surface pressure model for airfoil trailing-edge noise prediction, *Int. J. Aeroacoustics*, **14**, 833–882, (2015).

14. Herr, M., Ewert, R., Rautman, C., Kamruzzaman, M., Bekiropoulos, D., Arina, R., Iob, A., Batten, P., Chakravarthy, S. and Bertagnolio, F. Broadband trailing-edge noise predictions overview of BANC-III results, *21st AIAA/CEAS Aeroacoustics Conference*, p. 2847, (2015).

15. Drela, M. An analysis and design system for low Reynolds number airfoils, *Low Reynolds Number Aerodynamics*, Springer-Verlag, (2015).